Supplementary Figure Legends

Supplementary Figure 1. AngII activates SREBP-1. (A) MC were treated with AngII (100nM) for the indicated times and SREBP-1 activation assessed by immunoblotting of total cell lysate for the cleaved, mature form (mSREBP-1) (†$p<0.01$ vs con, n=6). **(B)** MC were treated with the indicated concentrations of AngII for 3h and SREBP-1 activation assessed by immunoblotting. **(C)** MC were transfected with the SREBP responsive plasmid SRE-GFP and treated with AngII for 3h. GFP expression, driven by SREBP activation, was demonstrated by immunofluorescence. **(D)** Intracellular lipid accumulation was assessed by Oil Red O staining after AngII for 24h.

Supplementary Figure 2. SREBP-1 transcriptional activation requires SCAP. The SCAP inhibitor fatostatin (20μM, 4h) blocked SREBP-1 transcriptional activation as assessed by quantification of GFP fluorescence in SRE-GFP transfected MC (†$p<0.01$ AngII vs others, n=8).

Supplementary Figure 3. SREBP-1 colocalizes to mesangial cells in AngII-treated glomeruli. Immunofluorescence staining of cortex from AngII-treated mice was performed for SREBP-1 with α-smooth muscle actin (αSMA) as a marker of activated mesangial cells, and DAPI as a marker of nuclei. Expression of SREBP-1 showed significant colocalization with mesangial cells (yellow) and with DAPI in nuclei (purple).

Supplementary Figure 4. The EGFR is not required for ER stress induction by AngII. AngII (30min)-induced eIF2α phosphorylation was not affected by the EGFR inhibitors PD168393 (0.5μM, 30min) or AG1478 (1μM, 30min).

Supplementary Figure 5. ER stress is required for SREBP-1 transcriptional activation. Both ER stress inhibitors 4-PBA (5mM, 2h) and salubrinal (30μM, 1h) blocked SREBP-1 transcriptional activation as assessed by quantification of GFP fluorescence in SRE-GFP transfected MC (†$p<0.01$ AngII vs others, n=9).

Supplementary Figure 6. PI3K/Akt activation upstream of SREBP-1 activation is also regulated by ER stress. Akt activated by the ER stress inducer thapsigargin (Tg, 200nM, 30min) was blocked by PI3K inhibition with LY294002 (20μM, 30min) or wortmannin (100nM, 60min).

Supplementary Figure 7. SREBP-1 mediates AngII induction of TGFβ1. MC were treated with AngII for 24h. **(A)** The S1P inhibitor AEBSF (500μM, 1h) inhibited AngII-induced TGFβ1 promoter luciferase activation (‡$p<0.001$ AngII vs others, n=9). **(B)** MC were transfected with control or SREBP-1 siRNA and efficacy of SREBP-1 downregulation assessed by immunoblotting. Expression of both precursor SREBP-1 (pSREBP-1) and the mature form of SREBP-1 (mSREBP-1) is inhibited.

Supplementary Figure 8. SREBP-1 mediates AngII-induced Smad3 activation. MC were treated with AngII for 24h and Smad3 transcriptional activity assessed using $CAGA_{12}$-luciferase. SREBP-1 inhibition with fatostatin (20μM) prevented AngII-induced Smad3 activation (*$p<0.05$, n=3).

Supplementary Figure 9. Fatostatin attenuates proteinuria induced by AngII. (A) Urine albumin, normalized to creatinine, was elevated in AngII-treated mice, and this was decreased by fatostatin (†$p<0.01$ vs others). **(B)** Fatostatin did not decrease the AngII-induced elevation in serum creatinine (†$p<0.01$ vs con).

Supplementary Figure 10. TGFβ1 colocalize to mesangial cells in AngII-treated glomeruli. Immunofluorescence staining of cortex from AngII-treated mice was performed for TGFβ, with α-smooth muscle actin (αSMA) as a marker of activated mesangial cells. TGFβ showed significant colocalization with mesangial cells (yellow).

Supplementary Figure 11. AngII-induced TGFβ1 and matrix upregulation *in vivo* are inhibited by fatostatin. (A-C) Mouse kidney cortical sections were analysed by quantitative RT-PCR. Fatostatin inhibited AngII-induced upregulation of TGFβ1 (*$p<0.05$ vs others), collagen 1α1 (†$p<0.01$ vs others), and fibronectin (†$p<0.01$ vs con and fato, ‡$p<0.001$ vs AngII+fato).

Supplementary Figure 12. Fatostatin attenuates AngII-induced tubulointerstitial fibrosis. Masson Trichrome staining was performed. Quantification was done for the AngII groups only since no interstitial fibrosis was seen in the control or fatostatin groups. Data are expressed as percentage of positive area stained for randomly taken images from the kidney cortex (†$p<0.01$ vs AngII).

Supplementary Figure 13. Glomerular SREBP-1 and GRP78 in models of hypertension. (A) IHC was performed for SREBP-1 or GRP78 on kidney cortex of Dahl salt-sensitive rats given normal or high salt. Quantification of glomerular staining in 5 randomly taken images is shown below (‡$p<0.001$). **(B,C)** IHC was performed for SREBP-1 or GRP78 on kidney cortex of uninephrectomized mice given normal water or implanted with a DOCA pellet and given 1% NaCl in their drinking water. Representative images from two mice are shown. Expression of neither GRP78 nor SREBP-1 was increased in DOCA/salt mice.

Supplementary Figure 1

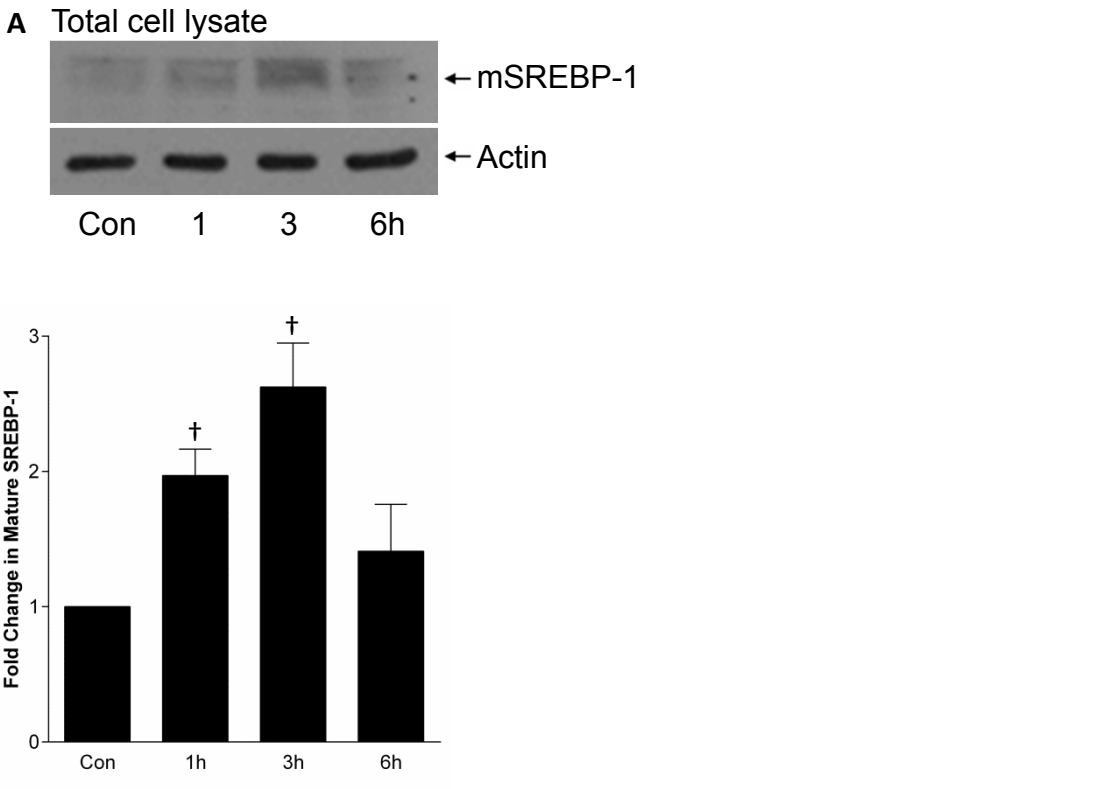

Supplementary Figure 1 continued

D Control Ang II

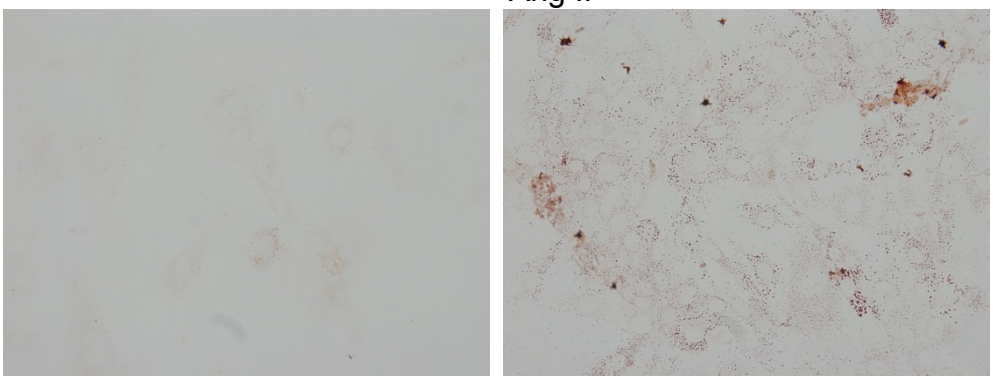

Supplementary Figure 2

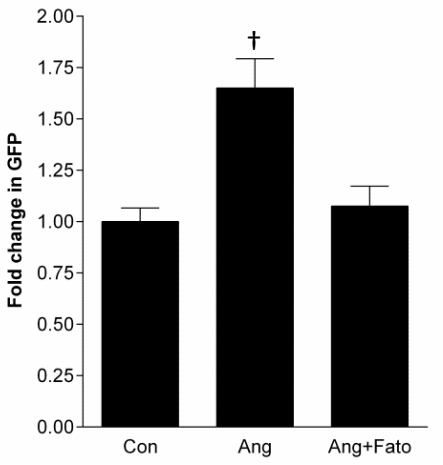

Supplementary Figure 3

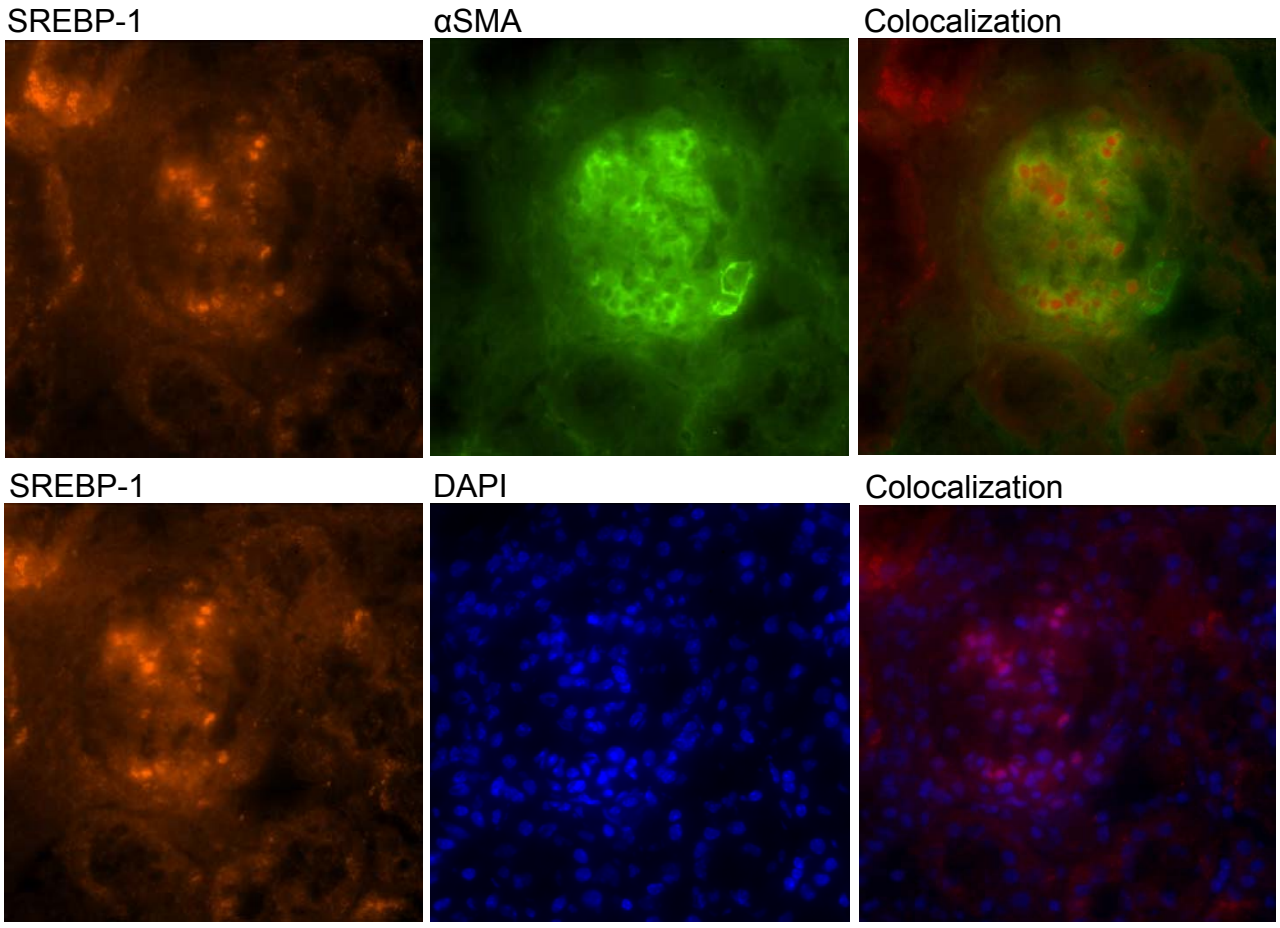

Supplementary Figure 4

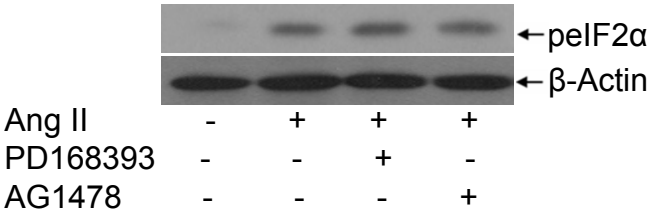

Supplementary Figure 5

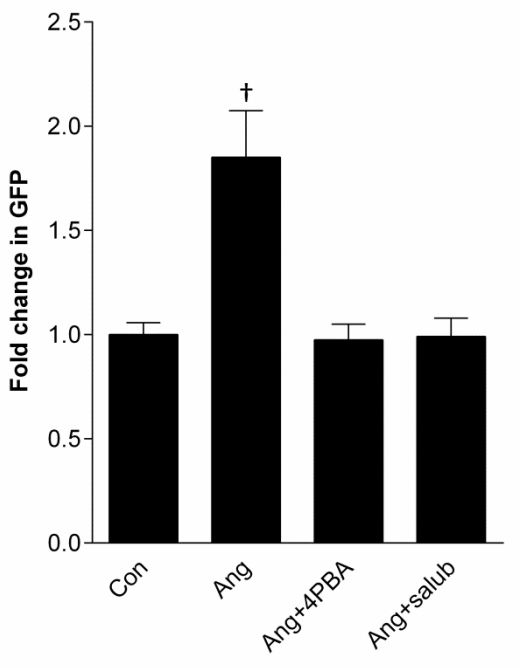

Supplementary Figure 6

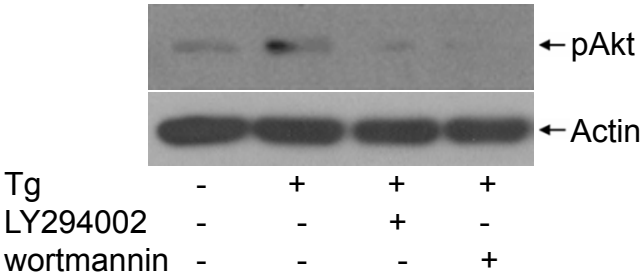

Supplementary Figure 7

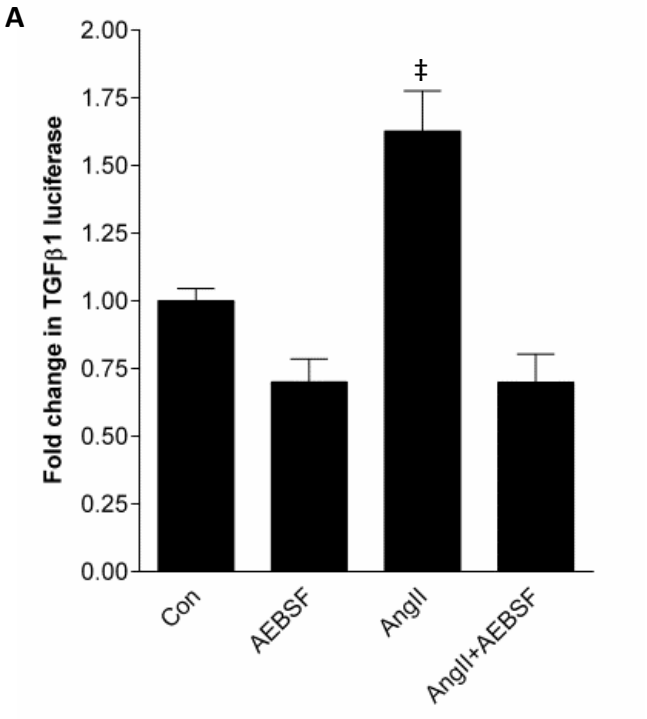

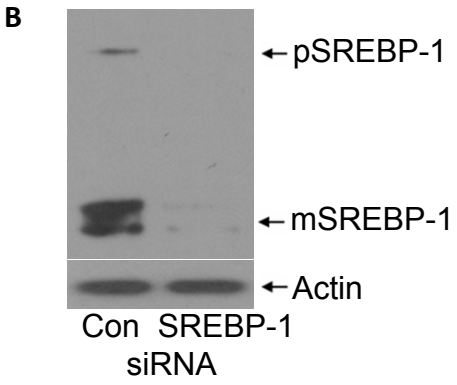

Supplementary Figure 8

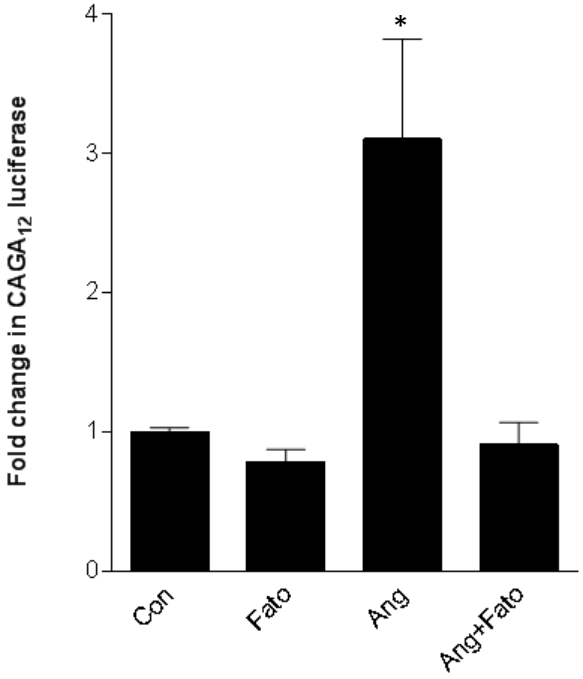

Supplementary Figure 9

A

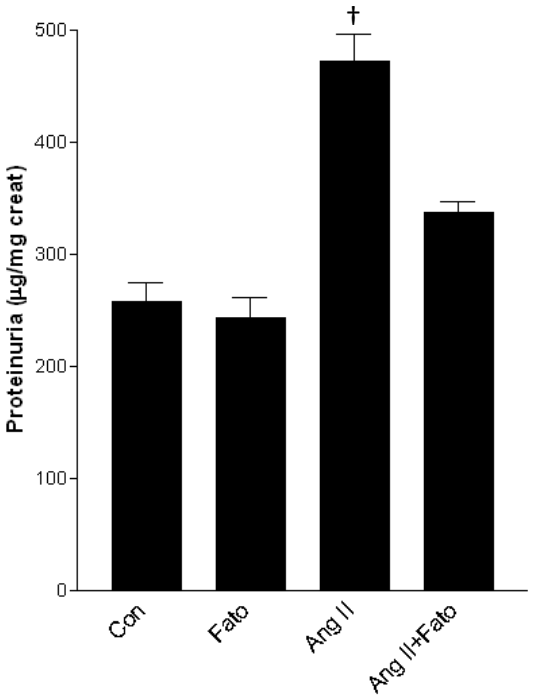

B

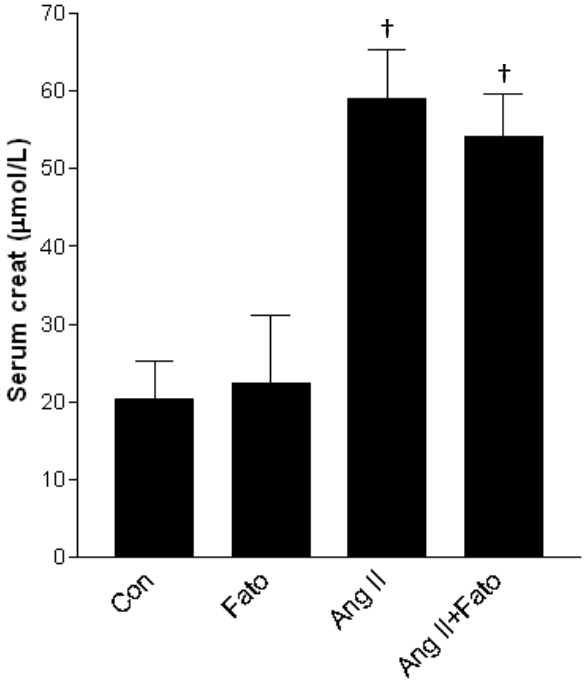

Supplementary Figure 10

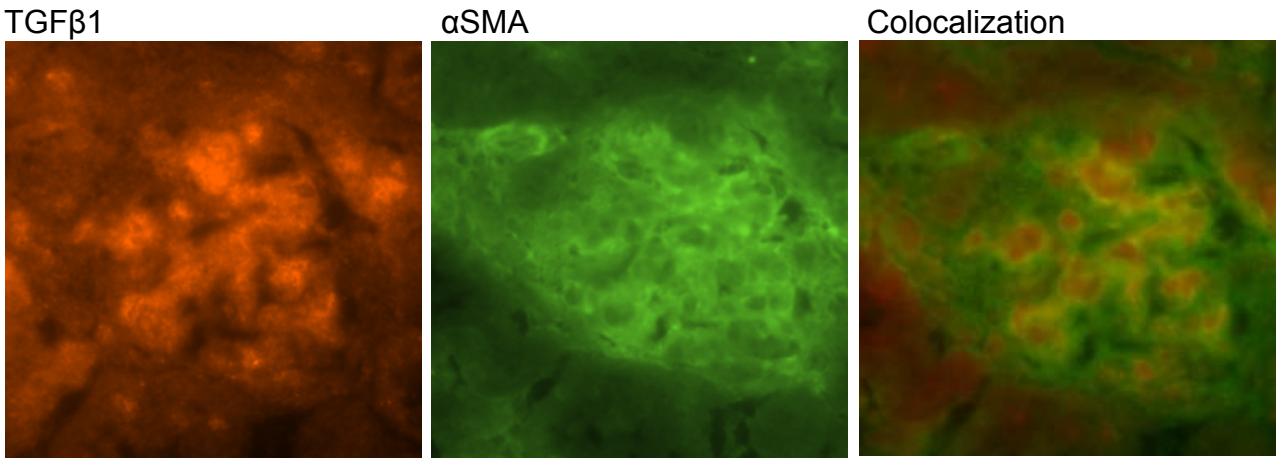

Supplementary Figure 11

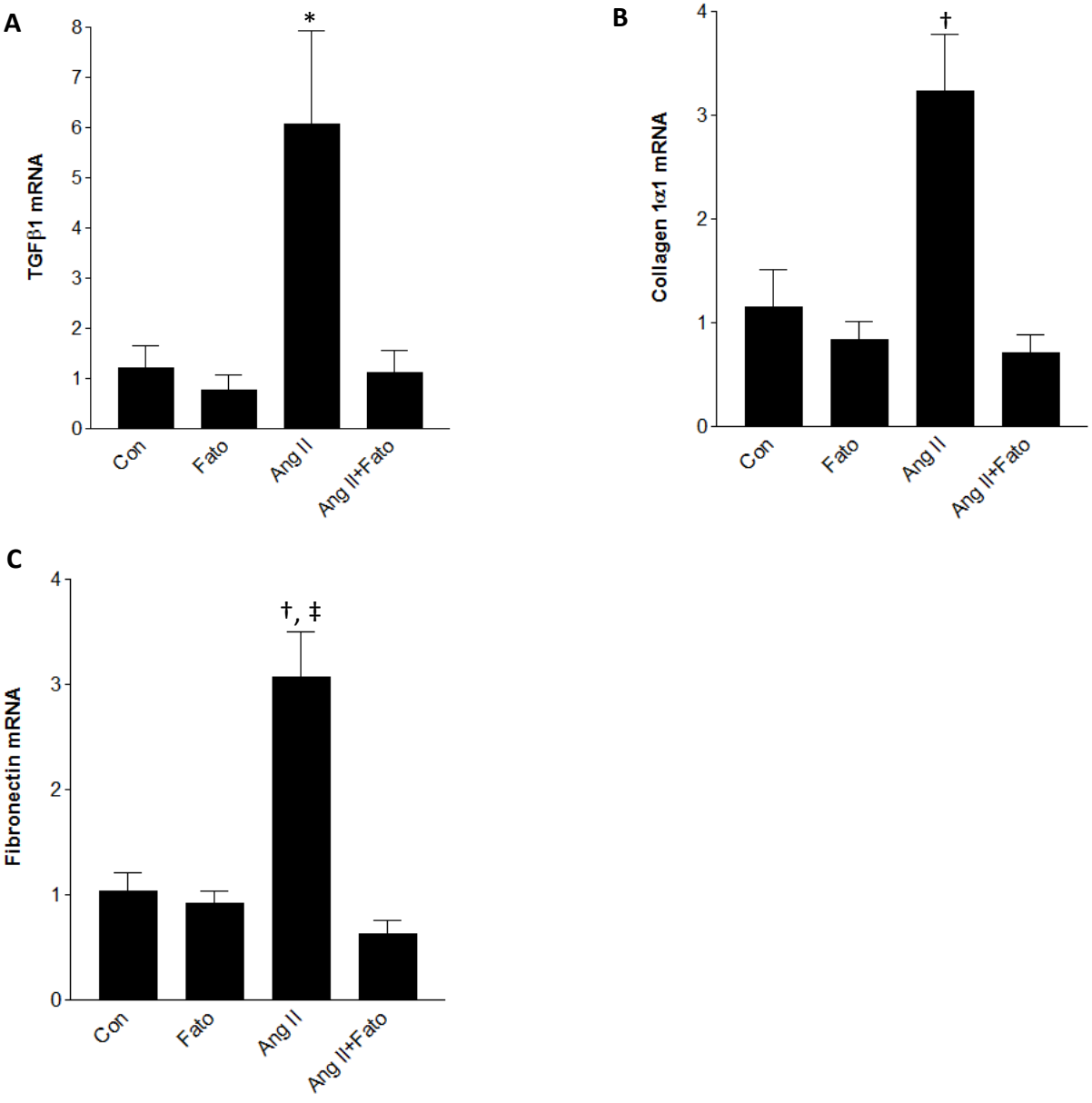

Supplementary Figure 12

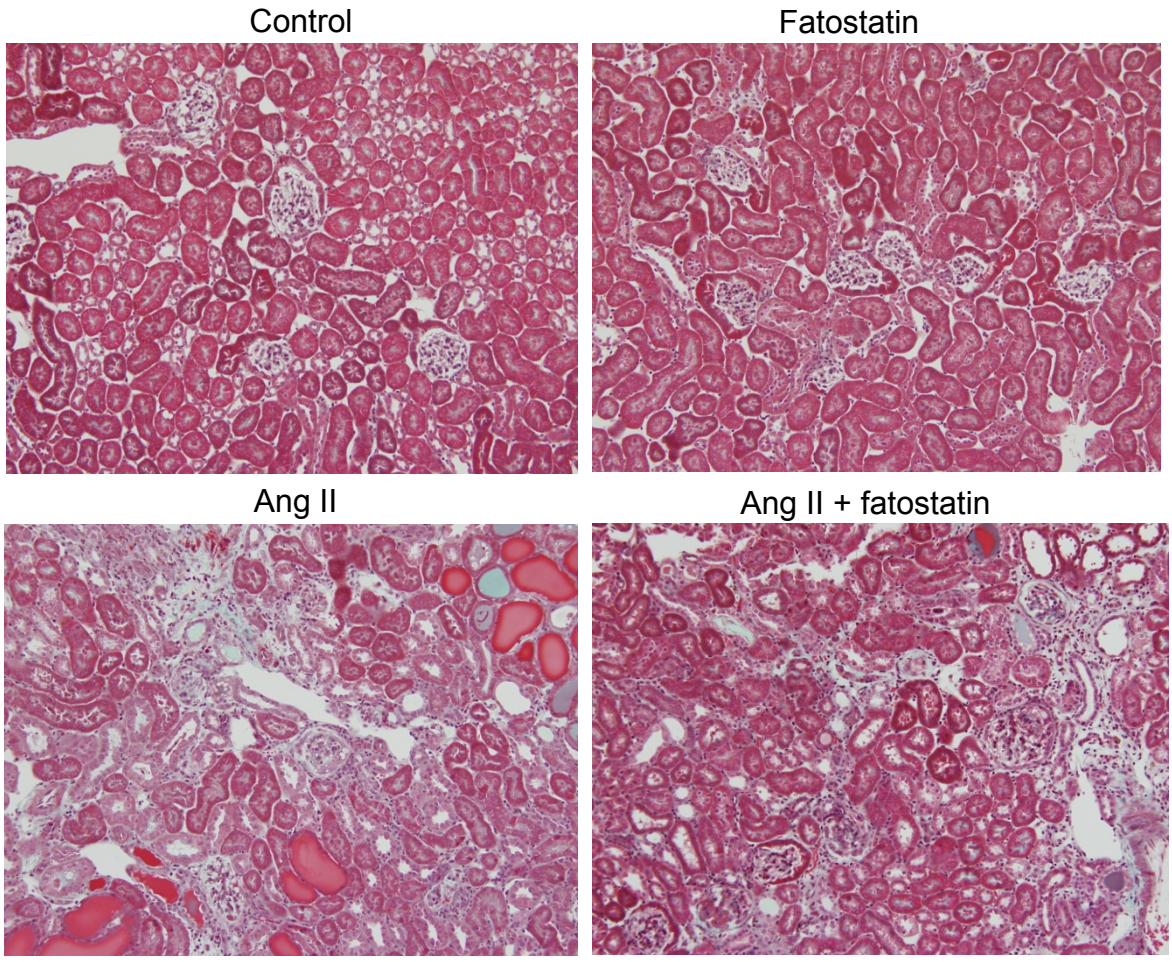

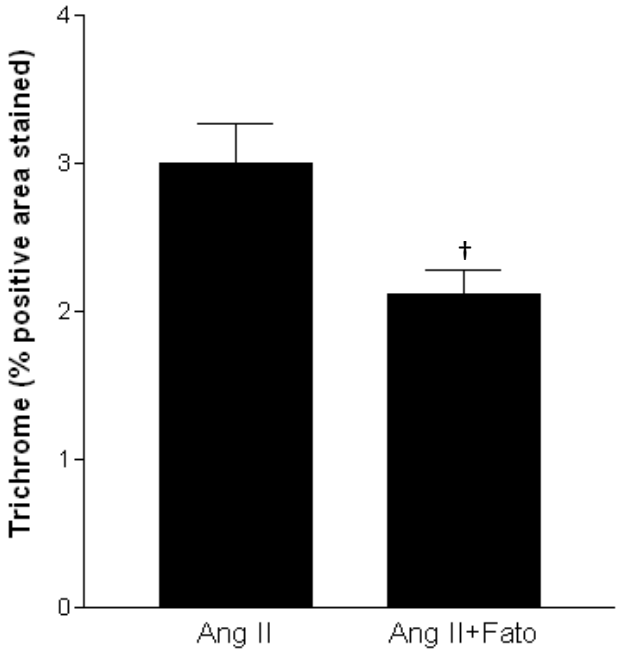

Supplementary Figure 13

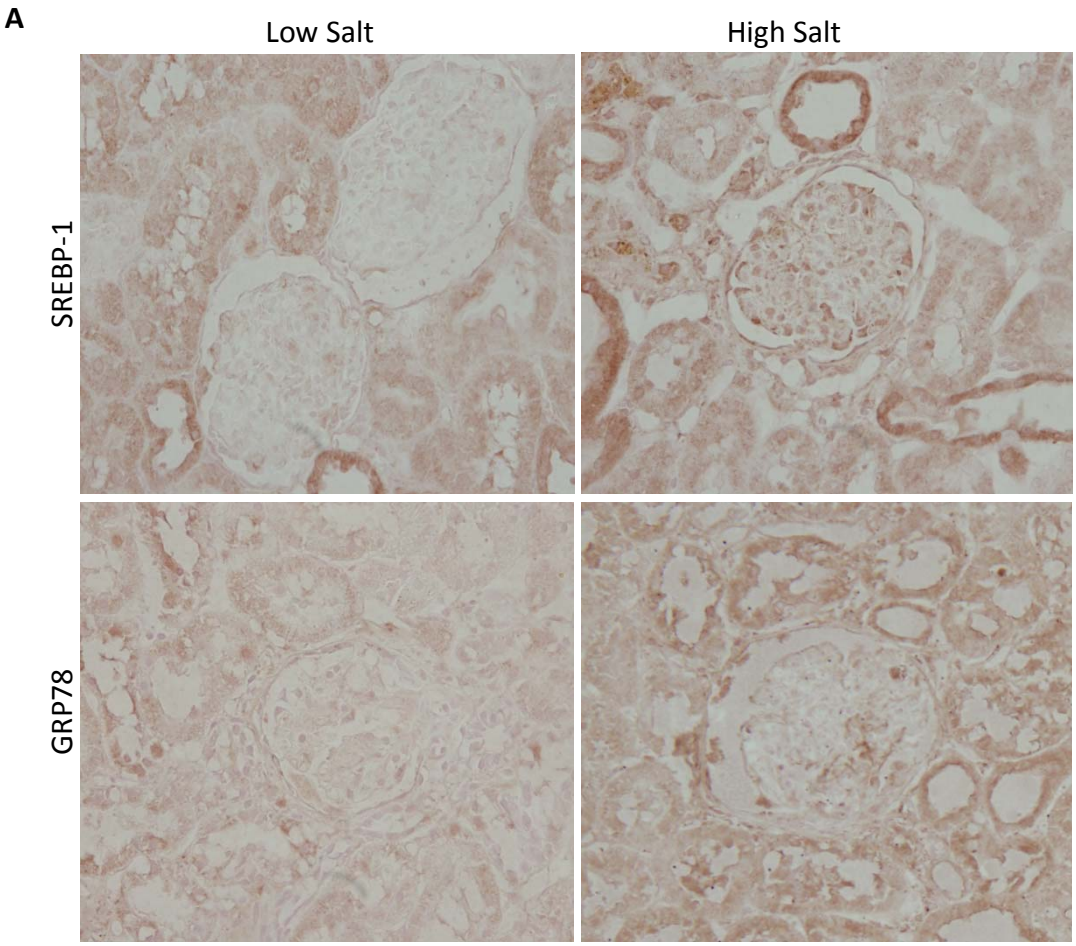

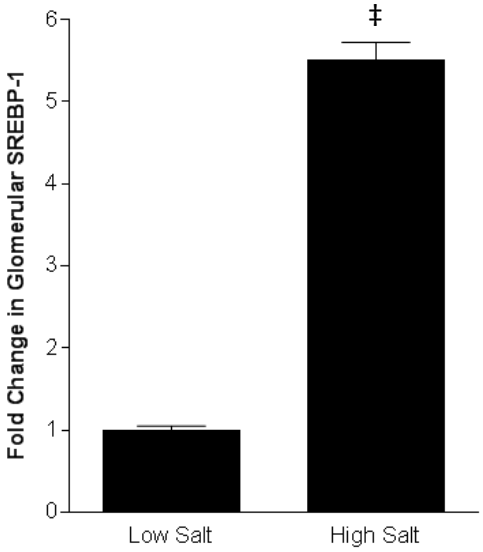

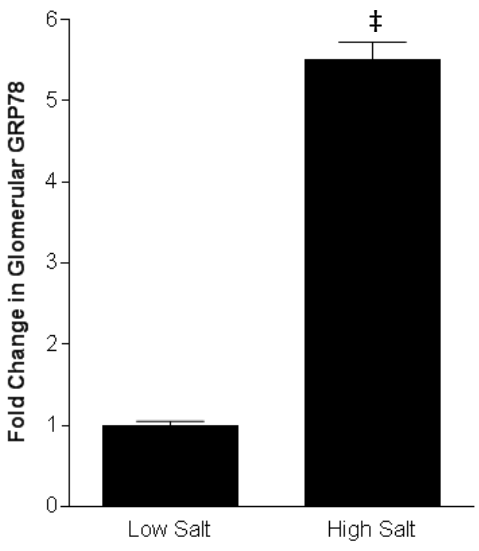

Supplementary Figure 13 continued